2026 IEEE/SICE International Symposium on System Integration (SII)
January 11-14, 2026. Cancún, México

Design of a Tendon-Driven Robotic Hand for High-Force Grasping and Dexterous Manipulation

Shinya Tajima[1] Jun Kinugawa[2]

Abstract— **Tele-operated systems are expected to play a vital role in environments that pose hazards to human workers and in scenarios where fully autonomous robots face significant challenges. The robotic hands incorporated into such systems must possess capabilities comparable to those of human operators to accomplish a wide range of tasks.**

In this study, we present the design and development of a tendon-driven robotic hand intended for integration into tele-operated systems. The target tasks encompass both dexterous manipulations and force-intensive operations typically performed by humans. To achieve these capabilities, we first defined the performance requirements necessary for task execution and analytically derived the link ratios that maximize gripping efficiency. From these, we further identified the link ratio that yields the largest operational workspace, thereby narrowing the range of suitable design parameters.

Based on the analytical findings, we devised an optimized link structure and tendon routing configuration tailored for tendon-driven actuation. A corresponding control system was implemented to operate the robotic hand and realize precise tendon-driven motion. Finally, we evaluated the system's ability to perform the designated tasks, demonstrating that the proposed robotic hand can effectively serve as a substitute for human operators in tele-operated applications.

I. INTRODUCTION

In hazardous environments such as outer space and radiation-contaminated areas, there is a growing demand for the deployment of advanced robotic technologies [1]-[3]. However, in situations where environmental conditions change rapidly and human judgment is required for each task, fully autonomous robots struggle to respond with sufficient flexibility. This has led to an increasing interest in tele-operated systems, which enable human operators to control robots from remote locations.

Currently, robotic hands in tele-operated systems are predominantly simple grippers with one or two degrees of freedom (DOF). While such mechanisms suffice for basic grasping tasks, precise manipulation of objects with diverse shapes demands hands with higher DOF.

In joint-actuated robotic hands, increasing the DOF inevitably results in larger and heavier structures [4]. Moreover, when introducing a tele-operated system into an existing human work environment, it is preferable for the robotic hand to maintain a size comparable to that of a human hand. Miniaturization, however, restricts the size of actuators that can be installed, which in turn limits the achievable output force. Therefore, there is a clear need for a robotic hand capable of performing both dexterous manipulation and force-intensive tasks, while preserving human-like dimensions. A schematic representation of the envisioned tele-operated system is shown in Fig.1.

One promising approach to meeting these requirements is the use of a tendon-driven robotic hand. In such hands, actuators and sensors can be mounted externally, enabling a more compact hand structure. This configuration allows for an increase in the number of actuators to achieve higher DOF or the use of larger actuators to generate greater force, without significantly increasing the size or weight of the hand itself.

However, tendon-driven robotic hands face two major challenges: tendon degradation and breakage and tendon elongation. If a tendon fails, force transmission is lost, resulting in a complete loss of control for the affected degree of freedom. Tendons also degrade gradually due to wear and repeated use, which increases the risk of sudden failure. Moreover, tendon elongation during operation leads to steady-state positional errors and dynamic delays in both winding displacement and transmitted tension. These effects make it difficult to precisely control joint angles and to regulate fingertip force with high accuracy, posing critical limitations for robotic hands intended to perform human-equivalent tasks.

The objective of this study is the development of a tendon-driven robotic hand capable of executing representative everyday tasks, including both force-intensive grasping and dexterous manipulation.

As an example of exerting grasping force using a tendon-driven robotic hand, Konda et al.[5] designed a tendon-driven robotic hand of human-comparable size and reported achieving a maximum grasping force of 72.0 N.

Furthermore, several studies have demonstrated the design

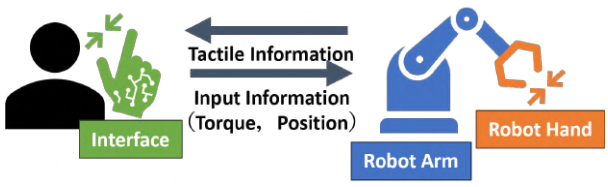

Fig. 1: Teleoperated system

This research was conducted with support from the Growth-Oriented Small and Medium Enterprises R&D Support Program (Go-Tech Program).

[1]Shinya Tajima is with the Department of Symbiotic Systems Science and Technology, Fukushima University, s2470031@ipc.fukushima-u.ac.jp

[2]Jun Kinugawa is with the Department of Symbiotic Systems Science and Technology, Fukushima University, kinugawa@sss.fukushima-u.ac.jp

Fig. 2: Bottle

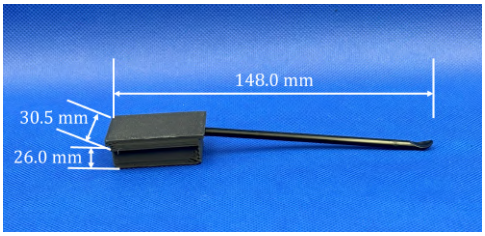

Fig. 3: Medicine spoon

of multi-degree-of-freedom tendon-driven robotic hands capable of grasping a wide variety of objects [6], [7], [8]. As one example, Ozawa et al.[9] implemented force control in a multi-DOF tendon-driven hand, enabling the hand not only to actively regulate the applied force but also to exploit the passive response of tendons to external forces. This capability allowed the hand to perform tasks such as deliberately slipping objects, thereby achieving object manipulation with a tendon-driven hand.

Previous studies have demonstrated tendon-driven robotic hands capable of either generating human-level grasping forces or performing dexterous manipulation. However, few examples exist in which both capabilities are achieved simultaneously within a hand of human-comparable size. Moreover, evaluations in prior work have often been limited to grasping a variety of objects. In this study, we conducted verification and evaluation of both grasping force and dexterity using well-defined tasks that simulate human activities.

The main contributions of this paper are summarized as follows:

1) Design of a tendon-driven robotic hand with human-comparable size and functionality
   We present a tendon-driven robotic hand that combines compactness with the capability to perform both forceful grasping tasks and dexterous manipulations, offering the potential to replace a range of daily human activities.
2) Verification through tasks simulating daily human activities
   Through tasks such as opening a bottle and manipulating rod-shaped objects, we verified that the proposed hand can exert substantial grasping force while also performing delicate manipulations.

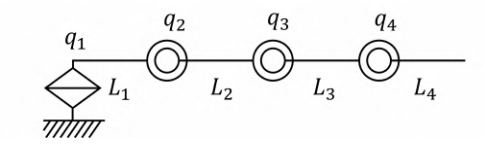

Fig. 4: schematic diagram of finger

II. DESIGN REQUIREMENTS OF THE ROBOTIC HAND

In this study, opening a bottle was selected as a representative task requiring grasping force, and manipulating a rod-shaped object was chosen as a representative dexterous manipulation task. Bottle opening was selected because it requires sufficient gripping force to remove the cap, providing a suitable benchmark for assessing the hand's force-generation capability. In particular, bottles used in hazardous environments—such as radiation facilities or chemical laboratories are often tightly sealed to prevent leakage of contents. Accordingly, tightly sealed bottles will be employed in the evaluation experiments to simulate realistic operational conditions. Conversely, the manipulation of rod-shaped objects was selected because such objects often have an off-center center of gravity, making them unstable during handling. This instability demands accurate posture control, making the task an effective metric for evaluating the motion accuracy of the robotic hand. For the evaluation tools, a wide-mouth polyethylene bottle commonly used in scientific experiments (Fig.2) was selected for the bottle-opening task, and a medicine spoon (Fig.3) was selected as the representative rod-shaped object.

In this study, the number of fingers on the robotic hand was set to three, which are treated as the thumb, index finger, and middle finger. This choice is motivated by the fact that a two-fingered configuration makes it difficult to stably grasp the center of a bottle cap. Additionally, for tasks involving the holding and manipulation of a medicine spoon, using three fingers allows one finger to act as a pivot while the remaining two fingers grasp the object, thereby enabling manipulation while suppressing rotation and tilt. This configuration permits object manipulation using only the hand, even in environments where large arm movements are restricted. Furthermore, from the perspectives of cost reduction and simplification of components, adopting three fingers—rather than a five-fingered design closer to the human hand is considered a rational choice. Each finger was endowed with 4 degrees of freedom, similar to the human finger, to achieve a structure capable of adapting flexibly to various grasped objects. The joints are denoted as MP1, MP2, PIP, and DIP from the base. MP1 rotates in the adduction–abduction direction, while MP2, PIP, and DIP rotate in the flexion–extension direction. Although human fingers possess 2 DOF at the MP joint, replicating this in a robotic hand is technically challenging. Therefore, as illustrated in Fig.4, 2 DOF are allocated to links L1 and L2, resulting in a 4-link structure. All three fingers share an identical structure.

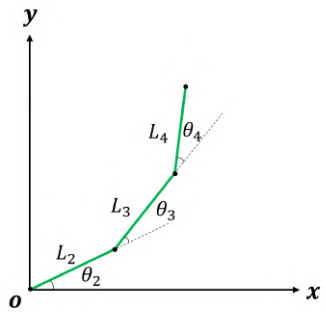

Fig. 5: 3 links on a 2-dimensional plane

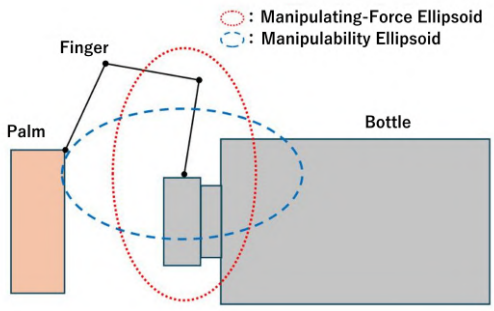

Fig. 6: Manipulation-force elipsoid and Manipulability elipsoid

III. Optimization Of Robotic Hand Link Ratios to Maximize Grasping Force

To determine the finger link ratio, we first consider the bottle-opening task. A three-fingered robotic hand requires a minimum fingertip force of $19.0\,\mathrm{N}$ per finger to open a bottle tightly closed by a human (Fig.2). In this study, the target gripping force was set to $57.0\,\mathrm{N}$ per finger by applying a safety factor of 3. To meet this target, the finger link ratio was selected to maximize the ease of generating fingertip force. For this analysis, a two-dimensional finger model with three links and 3 DOF was considered, as illustrated in Fig.5, where link L_1 (responsible for adduction–abduction) was omitted. Among possible link ratios, the evaluation criterion was the orientation of the major axis of the manipulating-force ellipsoid[10] at a given fingertip position, representing the direction in which force can be most easily applied. As shown by the dotted lines in Fig.6, link ratios were sought that oriented the major axis as close as possible to the direction perpendicular to the bottle surface, while also satisfying other design constraints and grasping requirements.

A. Calculation Conditions

1) The total finger length, excluding L_1, was fixed at $120.0\,\mathrm{mm}$ to match the dimensions of a human hand.
2) To achieve roughly uniform intervals within the feasible design range, other three link-length(L_2,L_3,L_4) ratios were selected from the set $1, 0.75, 0.5, 0.25$. This resulted in a total of 64 possible combinations being investigated.

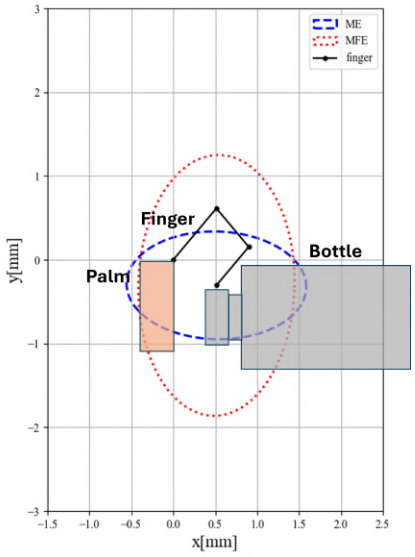

Fig. 7: Results (L2:L3:L4 = 0.75:1:1)

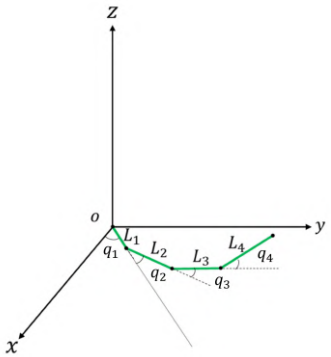

Fig. 8: 4 links on a 3-dimensional plane

3) The joint angle ranges during bottle gripping were set to $-\pi/6 < q_2 < \pi/2$, $-2\pi/3 < q_3 < 2\pi/3$, $-2\pi/3 < q_4 < 0$.
4) The position deviation from the lid radius of $29.0\,\mathrm{mm}$ was limited to within $\pm 1.0\,\mathrm{mm}$.
5) The minimum clearance between the fingertips and the palm was $10.0\,\mathrm{mm}$.
6) The angle between the fingertip direction and the DIP joint axis was constrained to be greater than $45°$ from the x-axis.
7) The major axis of the manipulating-force ellipsoid was required to be within $3°$ of the vertical direction.

B. Manipulability and Manipulating-Force Ellipsoid

For the three-link planar finger model in Fig.5, the fingertip position vector $\boldsymbol{p} = [x, y]^{\mathrm{T}}$ is expressed as

$$\boldsymbol{p} = \boldsymbol{f}(\boldsymbol{q}), \tag{1}$$

where $\boldsymbol{q} = [q_2, q_3, q_4]^{\mathrm{T}}$ is the joint angle vector. Differentiating with respect to time yields

$$\dot{\boldsymbol{p}} = \boldsymbol{J}\dot{\boldsymbol{q}}, \tag{2}$$

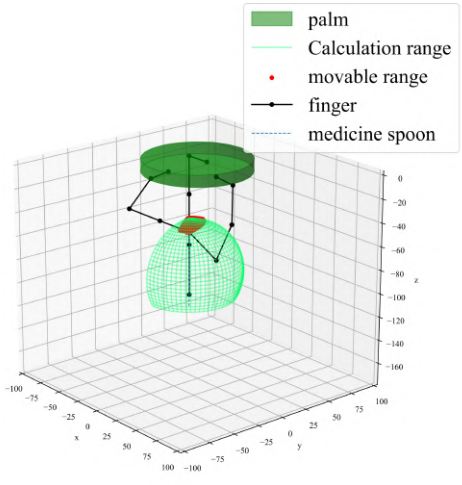

Fig. 9: $L_2 : L_3 : L_4 = 0.75 : 1 : 1$ calculation results

where $\boldsymbol{J}$ is the Jacobian matrix.

Let $\sin q_1$ and $\cos q_1$ be denoted as s_1 and c_1, respectively, and $\sin(q_1+q_2)$ and $\cos(q_1+q_2)$ be s_{12} and c_{12}, respectively. The Jacobian for the configuration in Fig.5 is given by

$$\boldsymbol{J} = \begin{bmatrix} -L_2 s_2 - L_3 s_{23} - L_4 s_{234} & -L_3 s_{23} - L_4 s_{234} & -L_4 s_{234} \\ L_2 c_2 + L_3 c_{23} + L_4 c_{234} & L_3 c_{23} + L_4 c_{234} & L_4 c_{234} \end{bmatrix} \tag{3}$$

Applying singular value decomposition (SVD), the Jacobian is expressed as

$$\boldsymbol{J} = \boldsymbol{U}\boldsymbol{\Sigma}\boldsymbol{V}^T \tag{4}$$

where $\boldsymbol{U}$ and $\boldsymbol{V}$ are orthogonal matrices of dimensions 2×2 and 3×3, respectively, and $\boldsymbol{\Sigma}$ is

$$\boldsymbol{\Sigma} = \begin{bmatrix} \sigma_1 & 0 & 0 \\ 0 & \sigma_2 & 0 \end{bmatrix} \tag{5}$$

Here, σ_1 and σ_2 denote the singular values of the Jacobian $\boldsymbol{J}$, corresponding to the two largest square roots of the eigenvalues of $\boldsymbol{J}^T\boldsymbol{J}$. Let the i-th column vector of $\boldsymbol{U}$ be $\boldsymbol{u}_i$. Each $\boldsymbol{u}_i$ indicates the direction of a principal axis of the corresponding ellipsoid.

- Manipulability ellipsoid:
  principal axes are $\sigma_1\boldsymbol{u}_1$ and $\sigma_2\boldsymbol{u}_2$.
- Manipulating-force ellipsoid:
  principal axes are $\boldsymbol{u}_1/\sigma_1$ and $\boldsymbol{u}_2/\sigma_2$.

In Fig.6, the dashed lines represent the manipulability ellipsoid, while the dotted lines represent the manipulating-force ellipsoid. Among all candidates, only those manipulating-force ellipsoids that satisfy the specified design constraints are considered in the link-ratio selection process.

C. Results

From the 64 link ratios calculated, 21 that met the conditions were selected. An example of a posture and operating force ellipsoid that achieves higher output is shown in Fig.7.

TABLE I: Number of plots of link ratio and operable range

L_2	L_3	L_4	Number of plots
1	1	1	601
1	0.75	1	387
1	0.75	0.75	365
1	0.75	0.5	367
1	0.5	1	150
1	0.5	0.75	75
1	0.5	0.5	0
1	0.25	1	0
1	0.25	0.75	0
1	0.25	0.5	0
0.75	1	1	862
0.75	0.75	1	650
0.75	0.5	1	377
0.75	0.5	0.75	320
0.75	0.5	0.5	282
0.75	0.25	1	0
0.75	0.25	0.75	0
0.75	0.25	0.5	0
0.5	0.75	0.75	889
0.5	0.5	0.75	673
0.5	0.25	0.75	267

Fig. 10: CAD of robotic hand

In Fig.7, it can be seen that the major axis of the operating force ellipsoid shown by the dotted line extends in the y axis direction. This allows a force to be applied perpendicular to the bottle cap from the finger.

IV. Optimization of Robotic Hand Link Ratios to Enable Dexterous Manipulation

Next, we consider the manipulation of a medicine spoon as a representative dexterous task. In this analysis, the middle finger and a fixed point on the spoon are held stationary, while the thumb and index finger manipulate the unfixed point. The link ratio is then selected based on the configuration that allows the largest reachable workspace for the moving point, which is assumed to correspond to greater dexterity.

A 4-link, 4DOF model in three-dimensional space is employed, as illustrated in Fig.8. The workspace of each finger is computed using inverse kinematics from the fingertip coordinates of the thumb and index finger. The link ratio that maximizes the reachable range of motion is chosen to enhance the hand‘s dexterous performance.

TABLE II: Specification sheet of the proposed robotic hand

Number of fingers	3
Degrees of freedom (per finger)	4
Link length	4
Maximum gripping force	57.0 N
Range of motion	MP1: Approx. 130 degrees MP2: Approx. 104 degrees PIP: 120 degrees DIP: 120 degrees
Material (1st link)	Stainless steel (SUS303)
Material (2nd to 3rd links)	Aluminum (A6061)
Material (4th link)	PLA & Silicone Rubber (Dragon Skin™)

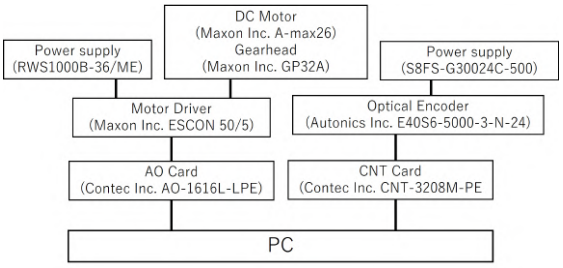

Fig. 11: System configuration

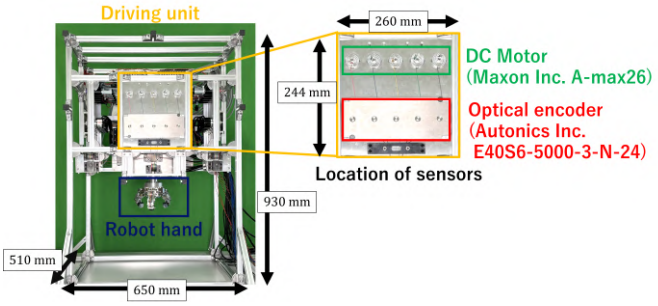

Fig. 12: Location of sensors

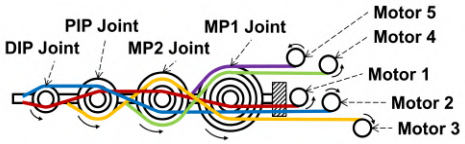

Fig. 13: Tendon arrangement

A. Calculation Conditions

The calculation conditions were defined as follows:

1) The total finger length was set to $120.0\,\mathrm{mm}$, consistent with the dimensions of a human hand.
2) With the palm center as the origin, the coordinates of the rotation axis of L_1 for the thumb, index, and middle fingers were set to $(x, y, z) = (23, 0, 0)$, $(-12, -20, 0)$, and $(-12, 20, 0)\,\mathrm{mm}$, respectively.
3) The joint angle ranges during spoon manipulation were set to $-2\pi/3 < q_2 < 0$, $-2\pi/3 < q_3 < 0$, and $-2\pi/3 < q_4 < 0$.
4) The range of motion for q_1 was set to $60°$ for the index and middle fingers and $90°$ for the thumb.
5) The fulcrum of the spoon was fixed at the midpoint of the middle finger's distal phalanx, and the grip position of the index and middle fingers was set $60.0\,\mathrm{mm}$ from the fulcrum.
6) The angle of the fingertips (distal phalanges) relative to the spoon was constrained between $90°$ and $18°$.

B. Results

As an example, the manipulating-force and manipulability ellipsoids for the link ratio $L_2 : L_3 : L_4 = 0.75 : 1 : 1$ are shown in Fig.9. The number of feasible configurations for each link ratio and the corresponding operable ranges are summarized in Table I. Based on these results, the optimal finger link ratio for the dexterous task of manipulating a medicine spoon was determined to be $L_2 : L_3 : L_4 = 0.5 : 0.75 : 0.75$.

The lengths of the finger links from the base were set to $22.5\,\mathrm{mm}$, $30.0\,\mathrm{mm}$, $45.0\,\mathrm{mm}$, and $45.0\,\mathrm{mm}$, respectively.

V. PROPOSED ROBOTIC HAND SYSTEM

Based on the design requirements and the finger link ratios determined to be optimal for bottle opening and spoon manipulation, a tendon-driven robotic hand was designed, as shown in Fig.10. The specifications of the robotic hand are summarized in Table II, and the overall system configuration is illustrated in Fig.11. An optical encoder (Autonics Inc., E40S6-5000-3-N-24) was employed to measure pulley displacement, while a DC motor with a reduction gear (Maxon Inc., A-max 26) served as the actuator. The arrangement of the sensors and actuators is depicted in Fig.12.

VI. OPERATION VERIFICATION

Tendon placement was determined following the methodology described by Ozawa et al. [11]. The adopted tendon configuration is shown in Fig.13. We implemented a joint-angle control system and evaluated the performance of the robotic hand through target tasks. We recognize the importance of evaluating joint-angle tracking accuracy and plan to address it in future work. However, at this stage, we adopted this approach because the ability to accomplish these tasks was considered a more appropriate measure of performance.

A. Bottle Opening Experiment

Each finger joint was controlled using inverse kinematics to apply a force perpendicular to the bottle cap. With the robotic hand exerting force on the cap, contact with the cap was confirmed by lowering the jack. Subsequently, the bottle was rotated manually to open it, allowing verification of whether the robotic hand could exert sufficient gripping force. The force required to close the bottle cap was measured using a force gauge and set to at least $3.5\,\mathrm{N \cdot m}$, corresponding to the typical force applied by a person when closing the cap tightly. Fig.14 illustrates the bottle opening process. The proposed tendon-driven robotic hand was confirmed to successfully open a tightly closed bottle cap.

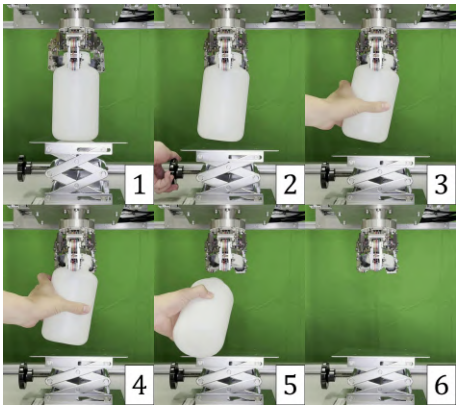

Fig. 14: Demonstration of bottle opening task using a tendon-driven robotic hand

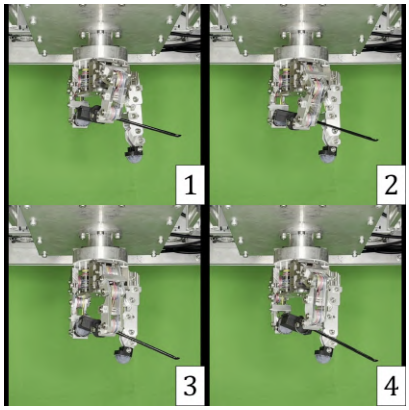

Fig. 15: Demonstration of medicine spoons handling task using a tendon-driven robotic hand

B. Medicine Spoon Operation Experiment

During the manipulation of the medicine spoon, the middle finger was fixed in an extended position and used as a fulcrum at the center of the spoon. The thumb and index finger grasped both ends of the spoon, and its posture was adjusted by moving these fingers. Fig.15 shows the spoon manipulation process. The results confirmed that posture control of the spoon was achievable using the proposed tendon-driven robotic hand.

VII. CONCLUSIONS

In this study, we confirmed that a tendon-driven robotic hand has the potential to perform everyday human tasks even in environments where performance is hindered by factors such as tendon elongation. Compared with other commercially available multi-DOF robotic hands such as the Shadow DEX-EE [12] and the Torobo Hand [13], the proposed hand demonstrates advantages in terms of size, grasping force and lightweight design of the movable part (Table III).

However, several issues affecting operational accuracy remain. First, tendon elongation and friction are not compensated, necessitating the development and implementation of a control method that accounts for tendon elongation. Second, tendon tension is not measured; thus, the incorporation of a feedback control system using tension sensors is planned. Third, the absence of fingertip force measurement results in open-loop control, limiting adaptability to external forces. This issue will be addressed by developing a radiation-resistant fingertip force sensor. Fourth, when integrating the robotic hand with a robotic arm, it will be necessary to redesign the enlarged actuation unit into a more compact form. Future work will focus on addressing these issues, integrating the robotic hand with a robotic arm, constructing a tele-operation system connected to a user interface, and conducting further operational verification. Finally, after integrating the robotic hand with a robotic arm and a user interface, further evaluations will be conducted to verify whether the system can perform a variety of everyday tasks beyond those examined in this study.

TABLE III: Comparison with Commercially Available Robotic Hands

	Proposed Robotic Hand	Shadow DEX-EE [12]	Torobo Hand [13]
Gripping force	Above 19 N	8 N	Approx.10 N
Overall length of the hand	193 mm	350 mm	240 mm
Weight of moving parts	Approx.1 kg	4.1 kg	Approx.2 kg

REFERENCES

[1] GITAI Japan Inc, https://gitai.tech/ (Accessed: Jul. 26, 2025)
[2] NASA, https://www.nasa.gov/robonaut2/ (Accessed: Jul. 26, 2025)
[3] HWM, https://www.hwm.com/telbot-166.html (Accessed: Jul. 27, 2025)
[4] T.Mouri, H.Kawasaki, K.Yoshikawa, J.Takai, and S.Ito, "Anthropomorphic Robot Hand： Gifu Hand Ⅲ," International Conference on Control Automation and Systems, pp.1288–1293, 2002.
[5] R. Konda, D. Bombara, S. Swanbeck and J. Zhang, "Anthropomorphic Twisted String-Actuated Soft Robotic Gripper With Tendon-Based Stiffening Ⅲ," in IEEE Transactions on Robotics, vol. 39, no. 2, pp. 1178-1195, April 2023.
[6] Minggao Guo, Yang Liu, and Yage Wang, "Design and Control of Tendon-Driven Dexterous Hands Ⅲ," Mechanical Design and Simulation: Exploring Innovations for the Future, pp. 93-103, 2025.
[7] Pasquale Chiacchio, Stefano Chiaverini, Lorenzo Sciavicco, and Bruno Siciliano, "Global Task Space Manipulability Ellipsoids for Multiple-Arm Systems Ⅲ," IEEE TRANSACTIONS ON ROBOTICS AND AUTOMATION, vol.7, no.5, 1991.
[8] L. Wen, Y. Li, M. Cong, H. Lang and Y. Du, "Design and Optimization of a Tendon-driven Robotic Hand Ⅲ," IEEE International Conference on Industrial Technology (ICIT), Toronto, ON, Canada, 2017, pp. 767-772.
[9] Ryuta Ozawa, Kazunori Hashirii, Yohtaro Yoshimura, Michinori Moriya and Hiroaki Kobayashi, "Design and control of a three-fingered tendon-driven robotic hand with active and passive tendons Ⅲ," Autonomous Robots, Vol 36, no.1-2, January 2014.
[10] C. Melchiorri, "Force manipulability ellipsoids for general manipulation systems Ⅲ," IFAC Proceedings, vol.27, pp.235–240, 1994.
[11] Ryuta Ozawa, Hiroaki Kobayashi, and Kazunori Hashirii, "Analysis, Classification, and Design of Tendon-Driven Mechanisms," IEEE TRANSACTIONS ONROBOTICS, vol.30, no. 2, pp.396–410, 2014.
[12] Shadow Robot Company Ltd.: "Shadow DEX-EE," Available at: https://shadowrobot.com/DEX-EE/, (Accessed: Nov. 6, 2025).
[13] Tokyo Robotics Inc.: "Torobo Hand," Available at: https://robotics.tokyo/products/hand/, (Accessed: Nov. 6, 2025).